JOURNAL OF VIROLOGY, Apr. 2002, p. 4022–4033 Vol. 76, No. 8
0022-538X/02/$04.00+0 DOI: 10.1128/JVI.76.8.4022–4033.2002

Human T-Lymphotropic Virus Type 1 Oncoprotein Tax Promotes S-Phase Entry but Blocks Mitosis

Min-Hui Liang,[1] Thomas Geisbert,[2] Yao Yao,[1] Steven H. Hinrichs,[3] and Chou-Zen Giam[1]*

Department of Microbiology and Immunology, Uniformed Services University of the Health Sciences, Bethesda, Maryland[1]; Pathology Division, U.S. Army Medical Research Institute of Infectious Diseases, Fort Detrick, Maryland[2]; and Department of Pathology and Microbiology, University of Nebraska Medical Center, Omaha, Nebraska[3]

Received 18 October 2001/Accepted 7 January 2002

Human T-lymphotropic virus type 1 (HTLV-1) Tax exerts pleiotropic effects on multiple cellular regulatory processes to bring about NF-κB activation, aberrant cell cycle progression, and cell transformation. Here we report that Tax stimulates cellular G_1/S entry but blocks mitosis. Tax expression in naive cells transduced with a retroviral vector, pBabe-Tax, leads to a significant increase in the number of cells in the S phase, with an accompanying rise in the population of cells with a DNA content of 4N or more. In all cell types tested, including BHK-21, mouse NIH 3T3, and human diploid fibroblast WI-38, Tax causes an uncoupling of DNA synthesis from cell division, resulting in the formation of multinucleated giant cells and cells with decondensed, highly convoluted and lobulated nuclei that are reminiscent of the large lymphocytes with cleaved or cerebriform nuclei seen in HTLV-1-positive individuals. This contrasts with the Tax-transformed cell lines, PX1 (fibroblast) and MT4 (lymphocyte), which produce Tax at high levels, but without the accompanying late-stage cell cycle abnormalities. PX1 and MT4 may have been selected to harbor somatic mutations that allow a bypass of the Tax-induced block in mitosis.

Human T-lymphotropic virus type 1 (HTLV-1) causes acute T-cell leukemia and lymphoma in a small percentage of infected individuals after a long latency period of up to 20 years. The mechanisms for viral reactivation from latency and viral cell transformation are not well understood but involve the unique viral transactivator-oncoprotein Tax. Tax serves two major functions during the viral life cycle: first, it mediates potent activation of viral transcription; second, it usurps regulatory mechanisms critical for cell activation and division to serve the metabolic needs of viral replication.

The mechanism by which Tax activates viral transcription is well understood. The viral transcriptional enhancer consists of three imperfect 21-bp repeats, each containing a cyclic AMP response element (CRE) core flanked by 5′ G-rich and 3′ C-rich sequences. The CREs in the 21-bp repeats are bound by the cellular basic domain-leucine zipper (bZip) transcription factors—CREB and ATF-1. CREB/ATF-1 and the 21-bp repeats, in turn, recruit Tax into stable ternary complexes (3, 55, 59, 65, 68, 69) in which Tax binds the basic domains of CREB/ATF-1 (1, 5, 48, 67) and makes contacts with the GC-rich sequences that flank the CRE, thus achieving the exquisite DNA sequence specificity of Tax-mediated long terminal repeat *trans*-activation (12, 28, 29, 34, 36, 47, 58, 66). In the context of the ternary Tax-CREB/ATF-1 21-bp repeat complex, Tax further recruits the coactivators CREB binding protein (CBP), p300, and a CBP-associated factor (P/CAF) for potent transcriptional activation (7, 18, 19, 23, 31, 34).

How Tax activates infected cells remains incompletely resolved. Tax perturbs many of the most fundamental functions of the cell, leading to potent activation of NF-κB (10, 17, 24, 61, 62), cell cycle dysfunctions (2, 13, 16, 32, 43, 44, 46, 52), cell transformation (14, 42, 50, 62), and others. Depending on the cell background, Tax has been reported to induce or prevent apoptosis (8, 9, 11, 60). Tax is also implicated in inactivating the functions of tumor suppressors p53 and p16 (35, 49, 56). More recently, Tax has been reported to (i) inhibit DNA repair (27, 33), (ii) cause clastogenic changes and micronucleus formation (37, 53), and (iii) induce aneuploidy and formation of binucleated cells by targeting the spindle checkpoint protein hsMAD1 (21, 25, 38). Many of the biological activities of Tax are likely to contribute to the leukemogenic process initiated by HTLV-1.

The lack of infectivity of cell-free HTLV-1 virions renders analyses of early events of HTLV-1 infection difficult. Many of the Tax-expressing HTLV-1 transformed T-cell lines were derived from patients with adult T-cell leukemia or HTLV-1-associated myelopathy or tropical spastic paraparesis after prolonged passage of their T lymphocytes in culture or by long-term cocultivation of X-irradiated HTLV-1-producing cells with primary cord blood or peripheral blood T lymphocytes (40). As a result, information regarding the initial effect of Tax on cells had not been well documented. Furthermore, for reasons not completely understood, stable expression of Tax in cultured cells, with a few exceptions, has been difficult to achieve, and it appears that Tax expression may be toxic to many cell types. Finally, a subgroup of transgenic mice expressing Tax develop thymic atrophy and die prematurely, whereas all surviving mice develop mesenchymal tumors (20, 42).

In this study, we use a Moloney murine leukemia virus (MuLV)-based retroviral vector, pBabe-puro (41), to transduce the *tax* gene into mammalian cells to examine the biological effects of Tax immediately after its expression. We found that Tax affects cell cycle progression at multiple levels;

* Corresponding author. Mailing address: Department of Microbiology and Immunology, Uniformed Services University of the Health Sciences, 4301 Jones Bridge Rd., Bethesda, MD 20814. Phone: (301) 295-9624. Fax: (301) 295-1545. E-mail: giam@bob.usuf2.usuhs.mil.

most importantly, it activates entry into S phase but delays mitosis. Tax causes a dramatic uncoupling of DNA synthesis from cell division, inducing the formation of multinucleated giant cells and large cells containing nuclei with convoluted and lobulated structure. This, however, is contrasted by the relative absence of late-stage cell cycle defects in an HTLV-1-transformed T-cell line, MT4, and a tumor cell line, PX1, derived from a *tax*-transgenic mouse (20, 42). MT4 and PX1 cells may contain specific somatic mutations selected to alleviate the block in mitosis induced by Tax. The Tax-mediated mitotic defects reported here add to the previously described DNA damages (clastogenic and aneuploidogenic changes) and cell cycle aberrations (increased G_1/S entry) inflicted by Tax.

MATERIALS AND METHODS

Plasmid construction. pBabe-puro (41), an MuLV-based retroviral vector, was used as to transduce the *tax* gene. The cDNA for wild-type Tax was derived by PCR using the Vent polymerase, cloned into pUC18 via *Bam*HI and *Eco*RI restriction sites, and confirmed by DNA sequence analysis. The *Bam*HI-*Eco*RI fragment was then inserted into pBabe-puro to produce pBabe-Tax. A consensus Kozak sequence, GCCACC, was incorporated immediately 5′ to the translational initiation codon of Tax for optimal protein expression. The oligonucleotide sequences for the upstream and downstream PCR primers are 5′-CGC GGA TCC GCC ACC ATG GCC CAC TTC CCA GGG TT-3′ and 5′-CGC GAA TTC TCA GAC TTC TGT TTC TCG GAA ATG T-3′, respectively.

Cell culture and medium. PA18G-BHK-21 (4); 293GP (generously provided by Viagene, Inc., San Diego, Calif.); NIH 3T3; human diploid fibroblast WI-38; and a fibroblast cell line, PX1, derived from a Tax-transgenic mouse were routinely cultured in Dulbecco's minimum essential medium (DMEM) supplemented with 10% heat-inactivated fetal bovine serum (FBS), penicillin and streptomycin (100 U/ml each), and 2 mM L-glutamine. HTLV-1-transformed cells (MT4) and Jurkat T cells were maintained in RPMI 1640 supplemented with 10% FBS and antibiotics at the same concentrations. PA18G-BHK-21, NIH 3T3, and WI-38 cells transduced with pBabe-Tax were selected in DMEM containing puromycin (1 g/ml) and 10% FBS.

Retroviral vector production. The packing cell line, 293GP, was derived from human embryonic kidney cell line 293. It produces MLV Gag and Pol proteins constitutively. The day before transfection, 293GP cells were plated at 10^5 cells per well on a six-well plate, with 2 ml of medium per well. Cells were grown to 70 to 80% confluency and transfected using Lipofectamine (GIBCO/Life Technologies, Gaithersburg, Md.). For each well of a six-well plate, 2 g of empty pBabe-puro vector or pBabe-Tax plasmid and 1 g of an expression plasmid, CMV-VSV-G, for the vesicular stomatitis virus envelope glycoprotein (VSV-G) were mixed with 11 μl of Lipofectamine to form the DNA-liposome complex. The mixture was incubated with the cells for 6 h at 37°C. Viral supernatants (500 ml each of pBabe-Tax and pBabe-puro) were collected at 24 and 48 h after transfection and centrifuged at approximately $300 \times g$ for 10 min to remove cells and debris and concentrated 1,000-fold to 0.5 ml using a Sorvall SS-34 rotor at 20,000 rpm for 2 h. Viral titer was determined using PA18G-BHK-21 cells and puromycin selection. The concentrated viral stocks had titers of approximately 10^9 infectious units per ml.

Transduction of *tax* gene into NIH 3T3, WI-38, and PA18G-BHK-21 cells and X-Gal staining. To determine the titer of pBabe-Tax viral stock, PA18G-BHK-21 cells were plated in DMEM medium on six-well plates at a density of 5×10^4 cells per well, 1 day before infection. After overnight growth, the cells generally reached about 20% confluency. Culture supernatants containing retroviral vectors in different dilutions were then added to the wells together with Polybrene (Sigma) at a final concentration of 8 g/ml. Infection was allowed to proceed for 4 h; after that the viral supernatant was removed and replaced with fresh medium. The cells were grown for 24 h and then subjected to selection in the same medium containing puromycin (1 g/ml). Cells were selected in puromycin for 1 week with one change of medium in between. Puromycin-resistant colonies appeared on the 7th or 8th day after the selection. To stain for β-galactosidase expression, the cells in each well of the six-well plate were washed once with 2 ml of phosphate-buffered saline (PBS), fixed with 0.2% glutaraldehyde–1% formaldehyde in 1 ml of PBS for 5 min at room temperature, washed twice with 2 ml of PBS each, and stained with 2 ml of X-Gal solution (PBS containing 2 mM $MgCl_2$, 4 mM potassium ferricyanide, 4 mM potassium ferrocyanide, and X-Gal [5-bromo-4-chloro-3-indolyl-β-D-galactopyranoside] [0.4 mg/ml]) at 37°C for 6 h. The number of puromycin-resistant colonies was used as a measure of the titer of the retroviral vectors. The titers of pBabe-Tax and pBabe-puro are routinely 10^5 to 10^6 infectious units per ml.

Electron microscopy. PA18G-BHK-21 cells were processed for transmission electron microscopy (TEM) according to conventional methods. Briefly, untreated and Tax-transduced cells were individually suspended in 3 ml of culture fluid, transferred to duplicate 1.5-ml conical Eppendorf microcentrifuge tubes, and loosely pelleted by centrifugation ($12{,}000 \times g$ for 30 s). Cell pellets were treated with 2% glutaraldehyde in 0.1 M phosphate buffer for 1 h and postfixed in 1% phosphate-buffered osmium tetroxide. Cells were stained en bloc with 0.5% uranyl acetate, dehydrated in ethanol and propylene oxide, and embedded in Poly/Bed 812 resin (Polysciences, Warrington, Pa.). Ultrathin sections were cut, placed on 200-mesh copper TEM grids, stained with uranyl acetate and lead citrate, and examined with a JEOL (Peabody, Mass.) 1200 EX transmission electron microscope.

Western blot analysis and immunofluorescence. Ten million puromycin-resistant PA18G-BHK-21 cells transduced with pBabe-Tax were washed with 5 ml of PBS twice, harvested by scraping in 5 ml of PBS, and collected by low-speed centrifugation. Total cellular proteins from each sample were extracted in 240 μl of RIPA buffer (10 mM Tris-HCl [pH 8.0], 150 mM NaCl, 0.5% NP-40, 0.1% deoxycholate, 1 mM EDTA, 1 mM phenylmethylsulfonyl fluoride, aprotinin [1 g/ml], leupeptin [2 g/ml]). Protein concentrations were determined by the Bradford assay. Typically, 50 μg of proteins was loaded and resolved on a sodium dodecyl sulfate–10% polyacrylamide gel for Western blot analysis. The proteins were then transferred to nitrocellulose membranes. The membranes were further incubated, using standard protocols, in a blocking solution containing 5% nonfat milk in PBS for 30 min and probed with a hybridoma antibody, 4C5 (1 to 50 dilution of the hybridoma supernatant in blocking solution), that reacts with the COOH-terminal region of Tax overnight at 4°C. The secondary horseradish peroxidase-conjugated, anti-mouse antibody (1:2,000) was from Santa Cruz Biotechnologies (Santa Cruz, Calif.). Immunofluorescence was performed as previously described (45) except that the 4C5 antibody was used in combination with a secondary rhodamine-conjugated donkey anti-mouse immunoglobulin G antibody (Jackson ImmunoResearch, West Grove, Pa.). The slides were mounted in a mounting medium containing 4′,6′-diamidino-2-phenylindole (DAPI; Vectashield; Vector Lab Inc., Burlingame, Calif.) and kept at 4°C in the dark. For MT4 cells which grow in suspension, eight-chamber culture slides (Nalge) were coated by adding 300 μl of a mixture of polylysine (1 mg/ml) and concanavalin A (1 mg/ml) in double-distilled H_2O to each slide and allowing them to sit undisturbed for 20 min at room temperature. The solution was then removed, and the slide was washed briefly twice with PBS. Cells were then cultured overnight in 10% CO_2 at low density in 300 μl of RPMI medium supplemented with 10% FBS (heat inactivated). An equal volume of a fixative solution (560 μl of 37% formaldehyde and 80 μl of glutaraldehyde in 18.6 ml of PBS) was then added to each well, and the slide was allowed to incubate undisturbed for 5 min at room temperature. The fixative was then removed, and the slide washed twice briefly with PBS. The immunofluorescence staining was carried out as described above.

Flow cytometry. PA18G-BHK-21 cells transduced with pBabe-Tax or pBabe-puro were harvested by scraping, collected by centrifugation, and washed twice with 2 ml of cold PBS. Approximately 3×10^6 cells were resuspended in 0.5 ml of PBS and fixed in 5 ml of 70% ethanol overnight at 4°C. The cells were then washed twice with 5 ml of cold PBS containing 0.5% bovine serum albumin and incubated for 30 min at 37°C in 0.5 ml of a solution containing propidium iodide (PI) (69 mM PI in 38 mM sodium citrate buffer; Boehringer Mannheim, Indianapolis, Ind.) and RNase (5 mg/ml). The cellular DNA content was determined by fluorescence-activated cell sorting (FACS) (EPICS XL-MCL flow cytometer; Beckman-Coulter). Data curves were fitted using the ModFit LT software package (Verity Software House, Inc., Topsham, Maine). To monitor the time course of Tax expression and cell cycle changes, PA18G-BHK-21 cells were first grown in DMEM containing 10% FBS, were serum starved for 48 h in DMEM containing 0.2% FBS, were infected with pBabe-puro or pBabe-Tax at a multiplicity of infection (MOI) of 10, and then were maintained in DMEM containing 20% FBS for various times. Cells were fixed and subjected to cell cycle analysis as described above.

BrdU labeling. PA18G-BHK-21 cells transduced with pBabe-Tax or pBabe-puro were labeled with 5-bromodeoxyuridine (BrdU) (30 μg/ml) for 1 h in DMEM containing 10% FBS under light-proof conditions. Two million cells were harvested by scraping and resuspended in 1 ml of PBS at room temperature. The cell suspension was rapidly injected into an ice-cold 70% ethanol fixative and incubated overnight at 4°C. Cells were pelleted at $300 \times g$ at 4°C for 5 min and then resuspended in 1 ml of an ice-cold solution containing 0.1% Triton X-100 and 0.1 M HCl for 1 min on ice. Cells were again pelleted for 5 min

at 300 × *g* at 4°C, washed in 5 ml of DNA denaturation buffer (0.15 mM NaCl, 15 μM trisodium citrate dihydrate), pelleted, and then resuspended in 1 ml of DNA denaturation buffer. To denature DNA, the cell suspension was heated for 8 to 10 min at 90°C and then placed on ice for 5 min. Five milliliters of freshly prepared dilution buffer (0.1% Triton X-100 and 1% bovine serum albumin in PBS) was added to the suspension, and the cells were pelleted by centrifugation for 5 min at 300 × *g* at room temperature. The supernatant was aspirated, and the cell pellet was gently vortexed in 100 μl of dilution buffer (PBS containing 0.1% Triton X-100 and 1% bovine serum albumin [wt/vol]). Twenty microliters of fluorescein isothiocyanate (FITC)-conjugated anti-BrdU antibody (FITC-conjugated mouse monoclonal antibody set; BD Bioscience, San Diego, Calif.) was then added and allowed to incubate for 30 min at room temperature in the dark. After antibody incubation, 5 ml of the dilution buffer was added into the cell suspension and cells were centrifuged for 5 min at 300 × *g* at room temperature. The cell pellet was then suspended in 1 ml of PI solution as described above, and incubated for 30 min at 37°C in the dark. Flow cytometry was performed to detect PI (red) and FITC (green) staining for nuclear DNA and BrdU content, respectively. FITC-conjugated mouse immunoglobulin G1 was used in place of anti-BrdU antibody as a negative control. Data curves were fitted using WinList software program (Verity Software House, Inc.).

RESULTS

HTLV-1 Tax is antiproliferative; Tax expression declines after cell passage. To facilitate efficient transduction of the *tax* gene into mammalian cells we inserted the cDNA of Tax as a *Bam*HI and *Eco*RI restriction fragment into the MuLV-based retroviral vector, pBabe-puro (41), to generate the pBabe-Tax vector (Fig. 1A). In pBabe-Tax, the *tax* sequence was engineered to contain a Kozak consensus preceding the translational start for optimal protein expression. Viral particles pseudotyped with VSV-G were then produced by cotransfection of pBabe-Tax with an expression plasmid, CMV-VSV-G (64), into an MuLV Gag- and Gag-Pol-expressing packaging cell line, 293GP. Culture supernatants containing the *tax* vector were then used to infect a baby hamster kidney (BHK) cell line, PA18G-BHK-21 (4), harboring a reporter cassette that comprises the *lacZ* gene under the control of the HTLV-1 long terminal repeat. The expression of LacZ in PA18G-BHK-21 is tightly regulated. No β-galactosidase activity could be detected in the absence of Tax. By contrast, when *tax* is introduced into the cell by DNA transfection or by retroviral vector-mediated transduction, potent expression of β-galactosidase is induced and can be readily scored by X-Gal staining. PA18G-BHK-21 cells were first infected with pBabe-Tax and then subjected to selection in medium containing puromycin for approximately 7 days. During this time, cells not transduced with the vector became eliminated by drug selection. Initially, puromycin-resistant colonies were individually picked, cloned, and expanded in culture. However, by the time each individual colony was grown to approximately 10^6 to 10^7 cells, Tax expression was no longer detectable (not shown). The progressive loss of Tax expression correlated with tissue culture passage of the entire population of puromycin-resistant cells freshly transduced with the Tax retroviral vector. One week following puromycin selection, abundant Tax expression could be detected (Fig. 1B, passage 0). However, with each subsequent passage, Tax expression became progressively reduced (Fig. 1B). These results suggest that Tax confers a proliferative disadvantage to the cells. This, of course, contrasts with the widely held suspicion that Tax plays a critical role in cell transformation and tumorigenesis.

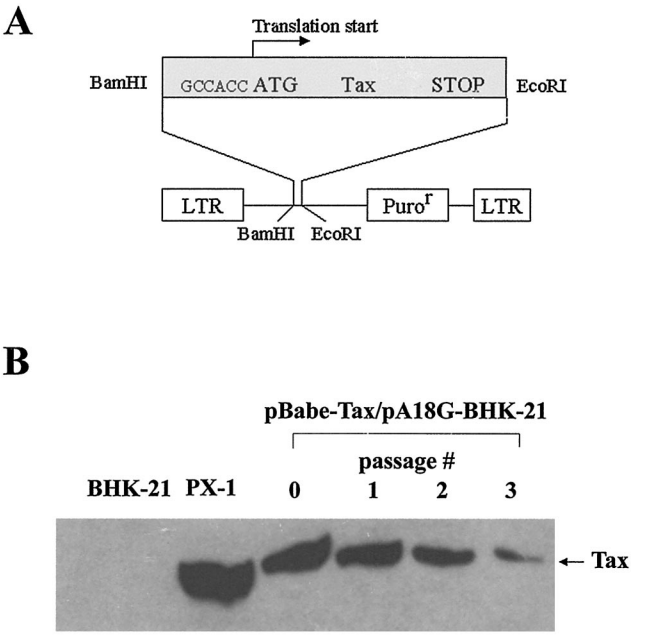

FIG. 1. (A) Construction of a Tax retroviral vector. The MuLV-based retroviral vector, pBabe-puro, was used to generate pBabe-Tax. A consensus Kozak sequence, GCCACC, was incorporated 5′ to the translational start codon of Tax. The complete coding sequence for Tax was then inserted into pBabe-puro via *Bam*HI and *Eco*RI restriction sites. LTR, long terminal repeat. (B) Tax expression declines rapidly with passage in cell culture. Tax-transduced PA18G-BHK-21 cells were passaged every 4 to 5 days. Immunoblot analyses were carried out using 4C5 hybridoma supernatant and 50 μg each of total proteins from cells transduced with pBabe-puro (lane BHK-21) or pBabe-Tax harvested after serial passages (passage 0 to 3). Tax-expressing PX1 cells were included as a control (lane PX-1). Tax expression was detected 1 week following puromycin selection (passage 0).

Tax expression results in formation of multinucleated giant cells. Unexpectedly, when *tax*-transduced PA18G-BHK-21 cells were examined under the microscope 1 week after puromycin selection, many giant cells—each containing an enlarged cytoplasm and multiple nuclei and with a concomitant loss of the elongated fibroblast-like morphology—were observed (compare Fig. 2A and B). These cells appeared flat and translucent. Their nuclei were clustered or strung together. The multinucleated giant cells as well as cells with double, greatly enlarged, and/or highly lobulated nuclei expressed Tax to high levels. This is revealed by the intense β-galactosidase color reaction after staining with X-Gal (Fig. 2A). In a given puromycin-resistant colony, the multinucleated cells that expressed Tax strongly (as indicated by X-Gal staining) were also surrounded by normal-looking cells that stained weakly with X-Gal (Fig. 2). We think the heterogeneity of the cell morphology is most likely due to the varied levels of Tax expression. Further confirmation of Tax expression in these cells was carried out by immunofluorescence using a monoclonal antibody, 4C5, which reacts with the COOH-terminal region of Tax (compare Fig. 3C and F). The nuclei in the multinucleated cells stained less brightly with DAPI and contained many unstained spots (Fig. 3E), suggesting their chromosomes may be decondensed. Interestingly, a significant fraction of Tax was found to localize to the cytoplasm of the multinucleated cells (Fig 3F). We also noticed from immunofluorescence staining

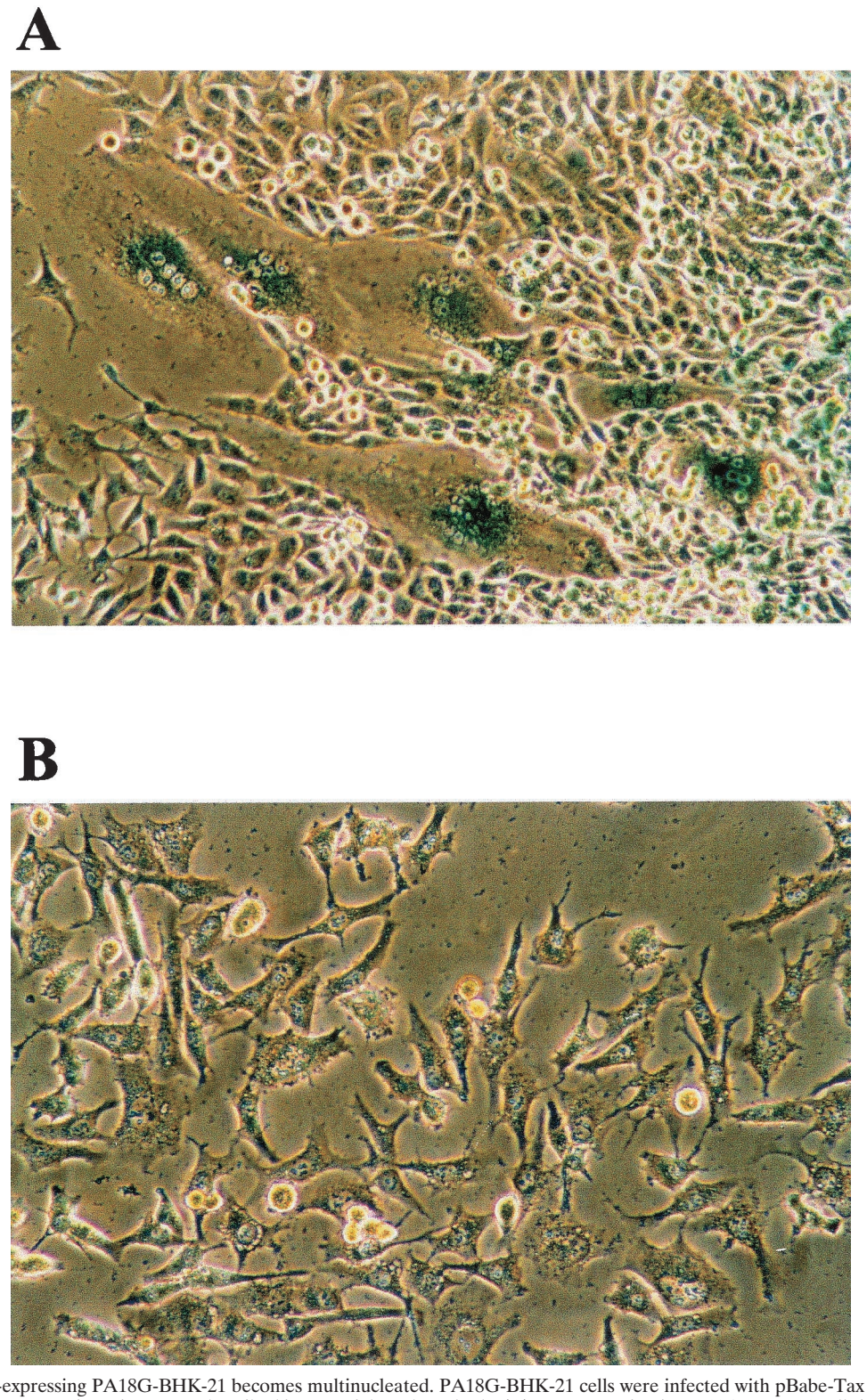

FIG. 2. (A) Tax-expressing PA18G-BHK-21 becomes multinucleated. PA18G-BHK-21 cells were infected with pBabe-Tax (A) or pBabe-puro (B) and selected for puromycin resistance as described in Materials and Methods. (A) Tax expression in PA18G-BHK-21 cells induces strong LacZ expression as revealed by X-Gal staining. Magnification, ×180.

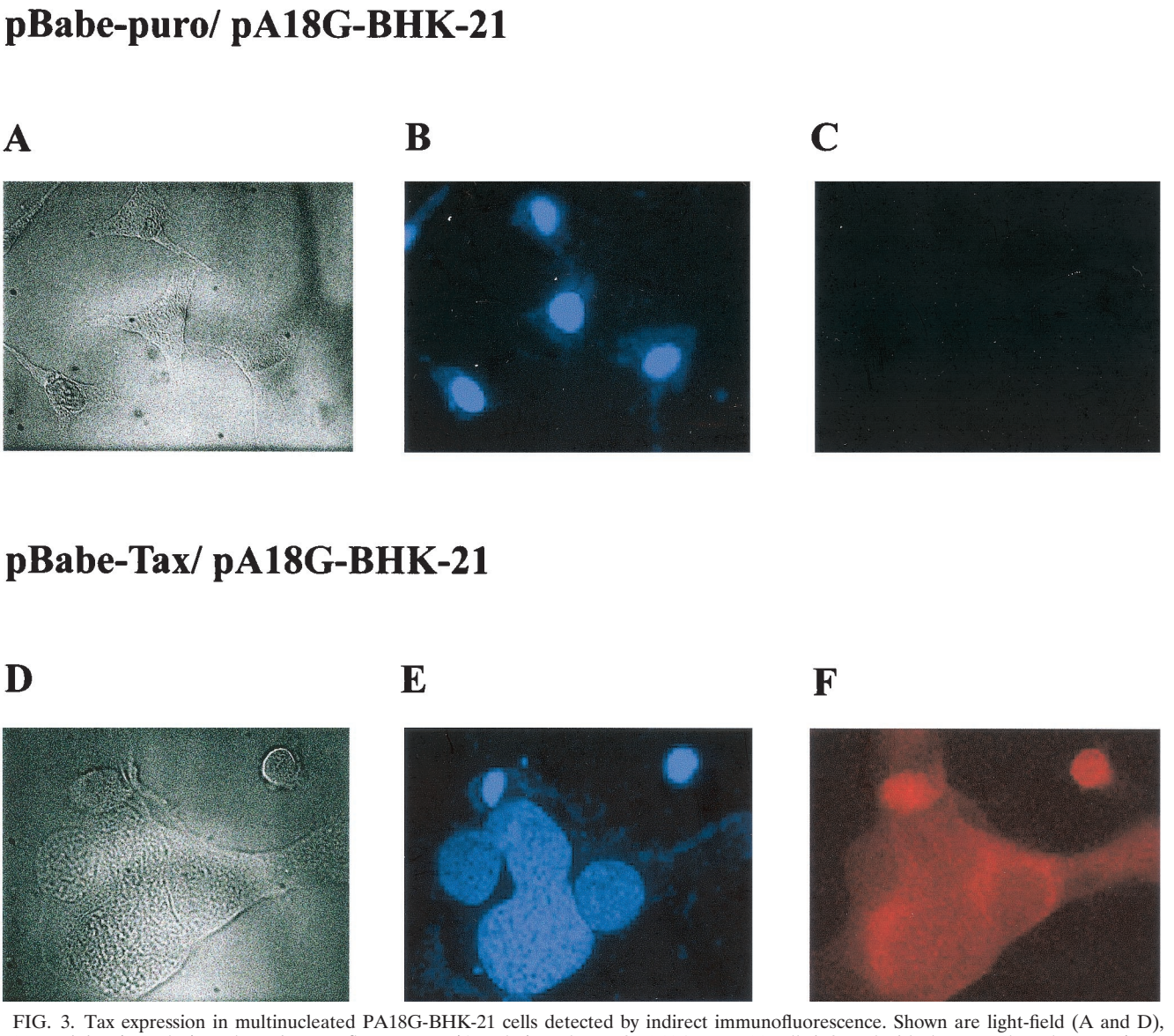

FIG. 3. Tax expression in multinucleated PA18G-BHK-21 cells detected by indirect immunofluorescence. Shown are light-field (A and D), DAPI staining (B and E), and Tax immunofluorescence (C and F) analyses of PA18G-BHK-21 cells infected with the control pBabe-puro (A to C) and the pBabe-Tax (D to F) retroviral vectors. A significant fraction of Tax in PA18G-BHK-21 localizes to the cytoplasm. Magnification, ×470.

that some cells expressed Tax in the nuclei. The significance for the differences in subcellular localization of Tax is not clear at present. Importantly, puromycin-resistant PA18G-BHK-21 cells infected with the control pBabe-puro retroviral vector did not become multinucleated (Fig. 3A to C). Therefore, the multinucleate cell phenotype seen here is caused by Tax expression rather than by trivial possibilities such as cell fusion caused by the VSV-G protein present on the surface of the retroviral vector used. To determine whether the cellular effects of Tax were limited to the PA18G-BHK-21 cells, the *tax* gene was also transduced into NIH 3T3 (mouse fibroblast) cells and human WI-38 (embryonic lung fibroblast) diploid cells. Indeed, following transduction of *tax* gene into these cells, similar nuclear and cellular abnormalities were also observed (Fig. 4A and B). These data suggest that Tax expression results in a defect in late stages of the cell division cycle, most likely at levels that include nuclear division and cytokinesis. These cell cycle defects explain the loss of Tax-expressing cells during passage.

Tax causes nuclear abnormalities and inhibits cytokinesis. To examine the cellular abnormalities of Tax-transduced PA18G-BHK-21 cells at a higher resolution, TEM was carried out. In agreement with the cytological changes seen with light microscopy, a comparison with the PA18G-BHK-21 cells transduced with pBabe-puro (Fig. 5A) revealed that the Tax-transduced cells contain an enlarged cytoplasm with abnormal or multiple nuclei (Fig. 5B and C). Particularly noteworthy are the highly convoluted but connected lobules of the nucleus in Fig. 5B and the three well-separated nuclei in Fig. 5C, which lend further support to the notion that Tax both induces nuclear abnormalities and inhibits cytokinesis. Finally, we also noticed that heterochromatin appears to feature less promi-

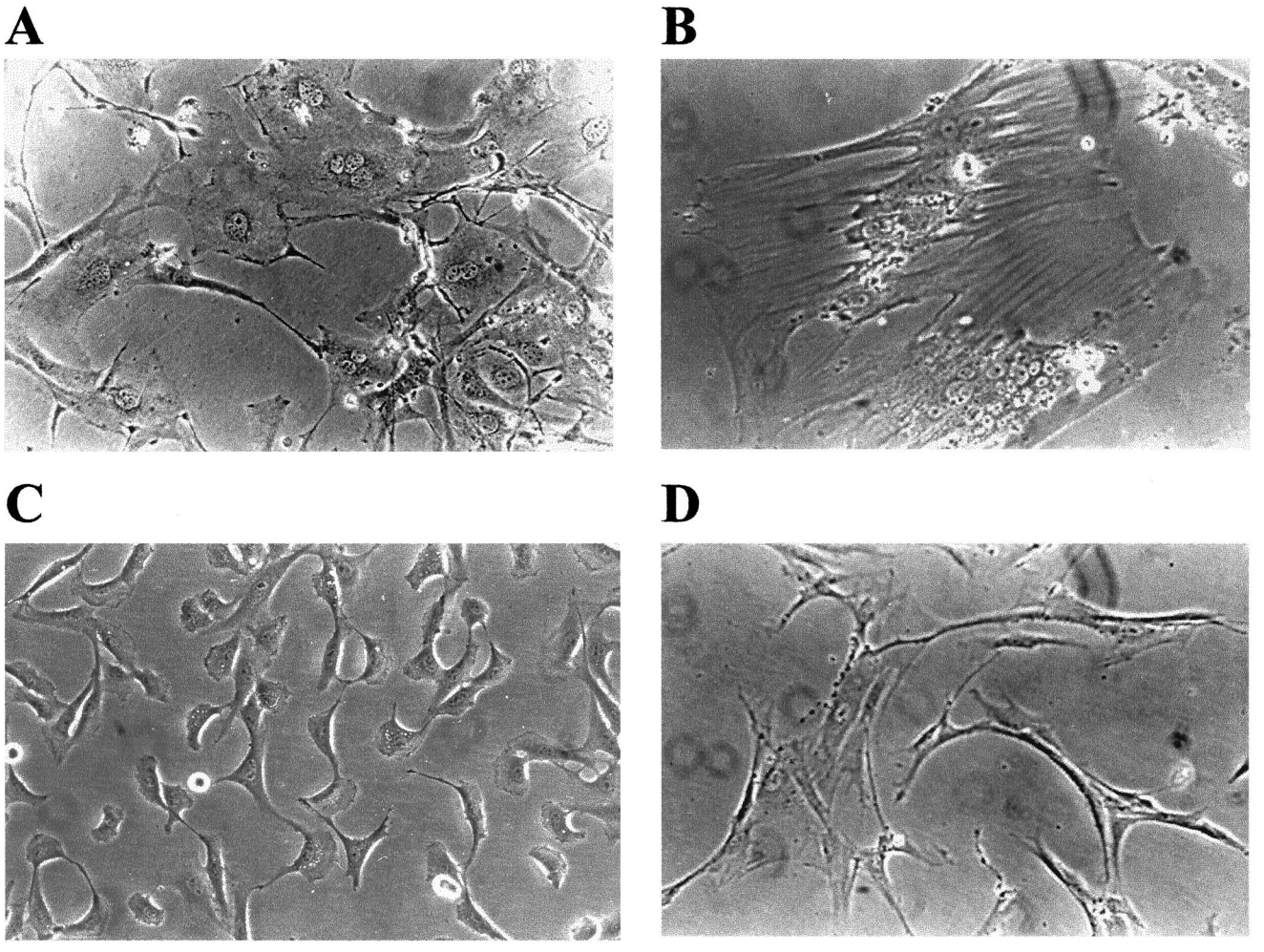

FIG. 4. Tax induces formation of multinucleated NIH 3T3 and WI-38 human diploid embryonic lung fibroblasts. NIH 3T3 cells transduced with Babe-Tax (A) and pBabe-puro (C) and WI-38 cells transduced with pBabe-Tax (B) and pBabe-puro (D) were derived as described in the legend to Fig. 2. Photographs (magnification, ×160) were taken 5 days after puromycin selection. (A and B) Note the multinucleated cells with enlarged cytoplasm.

nently in these abnormal nuclei, as suggested by the absence of dark, condensed materials at the periphery of the nuclear membrane--possibly one of the consequences of the potent activation of cellular signaling processes by Tax.

Tax expression increases G_1/S entry but delays mitosis. To examine the effects Tax exerts on cell cycle progression, we analyzed the pBabe-puro- and the pBabe-Tax-transduced PA18G-BHK-21 cells by flow cytometry. Tax- or vector-transduced cells were cultured under puromycin selection for 10 days. The puromycin selection was withdrawn on the 11th day, and the cells were harvested 24 h later for analysis. As shown in Fig. 6, 72, 16, and 12% of the cells in the pBabe-puro control were in the G_0/G1, S, and G_2/M phases of the cell cycle, respectively (Fig. 6A, the population in region R1 of the inset). In contrast, large populations of Tax-transduced cells were found in the S (32%) and G_2/M (29%) phases of the cell cycle, with a concomitant decrease in the fraction of cells in G_0/G1 (40%) (Fig. 6B, the cell population in region R1 of the inset). Consistent with the cytological observation, the pBabe-Tax population included readily detectable fractions of cells with 6N and 8N chromosome contents not seen in the control (compare Fig. 6A and B). Flow cytometry also revealed that many of the cells with 4N DNA content contain two distinct nuclei rather than a single nucleus with 4N DNA, as registered by the peak fluorescence signals which reflect peak DNA contents (vertical axis) and nuclear sizes (Fig. 6B, lower part of region R2 in the inset). Although two cells adhering to each other by aggregation would also be sorted into this population, we think many cells in this population were probably binucleated, as observed under the microscope. It should be noted that few cells in the control were in this condition (Fig. 6A). To confirm that Tax expression stimulates DNA synthesis, we labeled the pBabe-puro and the pBabe-Tax-transduced PA18G-BHK-21 cells with BrdU. As indicated in Fig. 7, significantly more pBabe-Tax cells (35%; $n = 5$) than pBabe-puro control cells (16%; $n = 6$) incorporated BrdU. Cell cycle effects of Tax were observed soon after retroviral transduction. In another set of experiments, we infected serum-starved, G_0/G1-arrested PA18G-BHK-21 cells with pBabe-Tax and pBabe-puro control vectors, respectively, at an MOI of 10, and monitored the

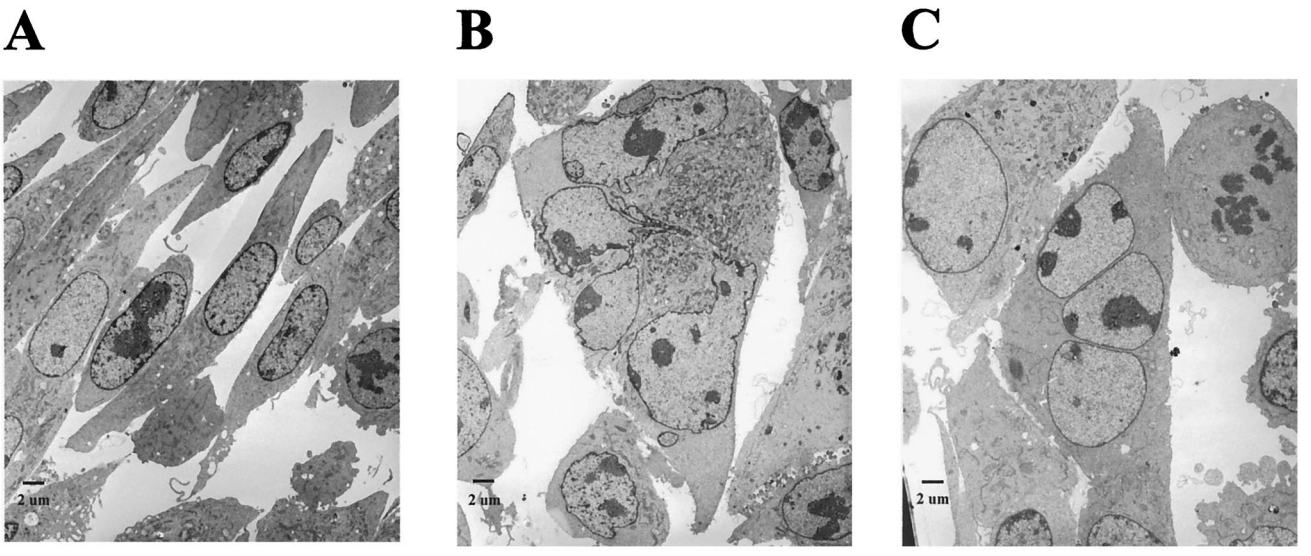

FIG. 5. Nuclear abnormalities and cytokinesis defects in Tax-transduced PA18G-BHK-21 cells. (A) Control pBabe-puro PA18G-BHK-21 cells. (B) Tax-transduced PA18G-BHK-21 cell with an enlarged cytoplasm and convoluted but connected nuclear lobules. (C) Tax-transduced PA18G-BHK-21 cell with three well-separated nuclei. Note that heterochromatin features less prominently in the abnormal nuclei in panels B and C, as suggested by the absence of dark, condensed materials at the periphery of the nuclear membrane.

infected cells by flow cytometry at different times. Tax-expressing cells emerge from G_0/G1 rapidly and in large numbers. As early as 24 to 48 h after pBabe-Tax transduction, many BHK cells began to enter into S phase, but they accumulated at G_2/M phase. These cell cycle effects became even more pronounced 72 h after transduction (Fig. 8). These results are consistent with the notion that although Tax activates cells to enter into S phase, it simultaneously causes a delay in G_2/M

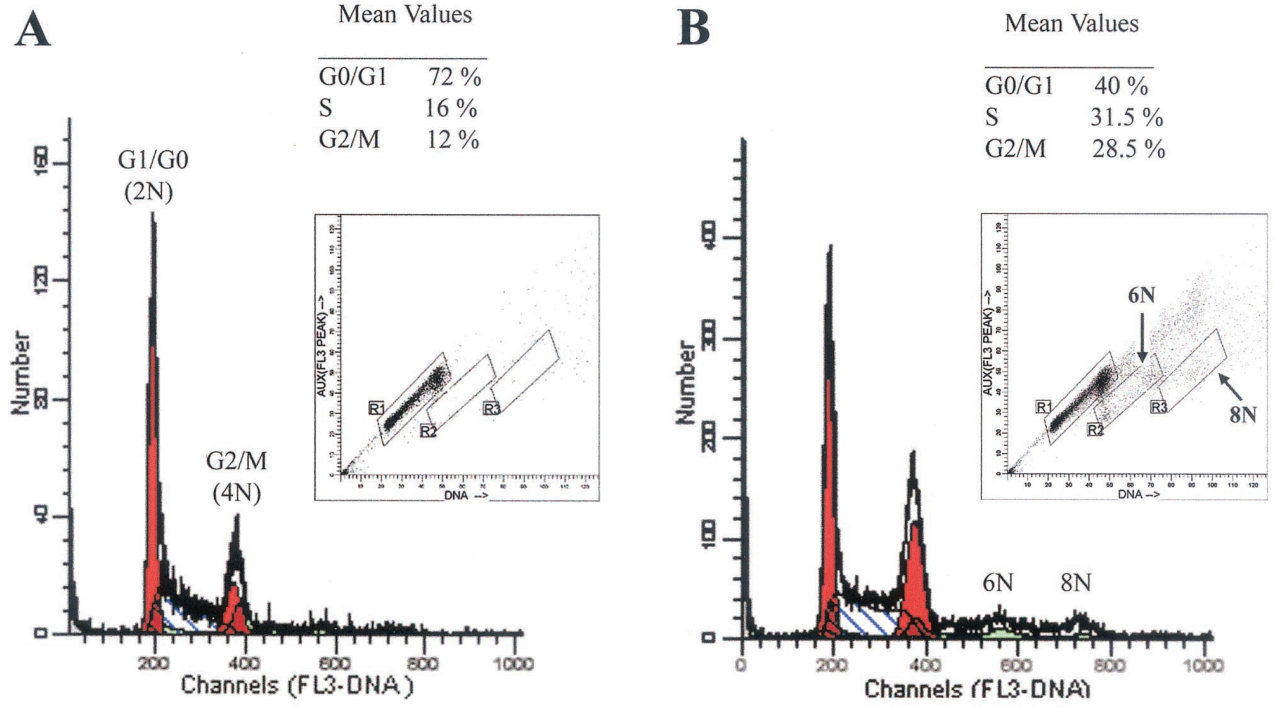

FIG. 6. Tax activates cells to enter into S phase but arrests them at G_2/M phase. PA18G-BHK-21 cells transduced with pBabe-puro (A) or pBabe-Tax (B) were placed under puromycin selection for 10 days and harvested for FACS analyses. Three million transduced cells were fixed in ethanol, stained with PI, and sorted by FACS. The DNA contents are as indicated. The inset in each panel shows the integrated total DNA content as reflected by total fluorescence signal (horizontal axis) and nuclear size as reflected by peak DNA content (vertical axis) of the total cell population analyzed. The cell number versus DNA content (regions R1, R2, and R3) was plotted. Mean values of the percentage of cells in different stages of cell cycle in R1 are indicated. Many pBabe-Tax-transduced cells were found to have a DNA content of more than 4N but with peak fluorescence of a single nucleus, consistent with the microscopic observation that they are multinucleated.

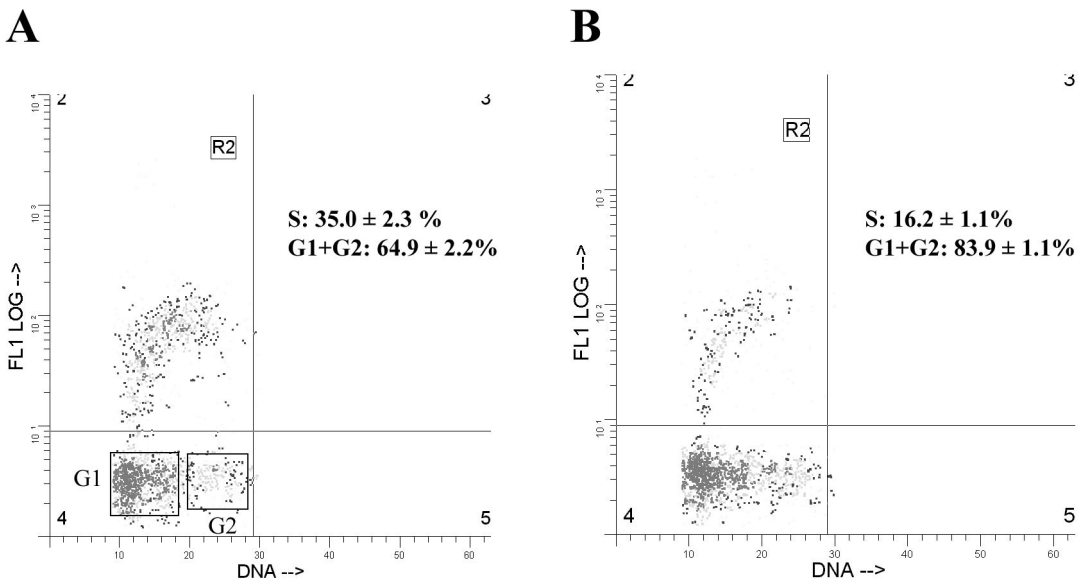

FIG. 7. Bivariate DNA and BrdU distributions in BHK cells transduced with pBabe-Tax (A) and pBabe-puro (B), respectively. The ordinate shows the BrdU incorporation detected with FITC-labeled monoclonal antibody; the abscissa shows the total DNA content detected with PI. Relative nuclear DNA and BrdU levels were computed using the WinList program. Region R2 denotes the cell population in S phase. The G_1 and G_2 populations are also boxed.

progression and/or a block in the completion of mitosis. The activation of S-phase entry coupled with a block in mitosis is most likely responsible for the great increase in DNA content in the multinucleated giant cells which simply continued to synthesize DNA in the absence of cell division. The enlarged nuclei and nuclear abnormalities seen in other cells probably reflect different degrees of cell cycle aberration caused by Tax. In aggregate, these data suggest that, in addition to activating G_1/S entry, Tax induces a block in the late stages of the cell division cycle in naive cells, at levels that include nuclear division and cytokinesis.

PX1 and MT4 are not G_2/M arrested and show no cytokinesis defect. With the dramatic cell cycle perturbation caused by Tax in mind, we examined two Tax-transformed cell lines, PX1 (a tumor cell line derived from a *tax*-transgenic mouse) and MT4, (an HTLV-1-transformed human $CD4^+$ T-cell line) for cell cycle defects. Interestingly, despite elevated levels of Tax expression, neither cell line exhibited any cell cycle difficulties (Fig. 9), suggesting that they may contain somatic changes that circumvent the cell cycle block, thus allowing the potent cellular stimulation initiated by Tax to be exploited for uncontrolled cell proliferation.

DISCUSSION

In this study, we provide evidence to show that HTLV-1 Tax expression causes cell cycle dysregulations that include activation of cellular entry into S phase followed by a block in mitosis. The effect of Tax on cell cycle is pleiotropic. Many Tax-expressing cells are bi-, tri-, or multinucleated (Fig. 2 to 5). The results described herein indicate that many of the Tax-expressing cells had slowed in completing or were unable to complete mitosis and/or cytokinesis. The loss of control over DNA replication and the failure to undergo proper cytokinesis and cell division as caused by Tax results in the formation of multinucleated giant cells and large cells with remarkably convoluted nuclear structure. The morphological features of the Tax-expressing cells in our experiments are reminiscent of the large lymphocytes with cleaved or cerebriform nuclei commonly called "flower cells" or "clover-leaf cells" that are often seen in HTLV-1-seropositive individuals (30, 51, 54, 57). The data presented here suggest that HTLV-1 Tax is most likely responsible for such nuclear and cytoplasmic abnormalities. It should be pointed out that these abnormalities, although frequently seen in HTLV-1-positive individuals, have not yet been correlated with specific sequelae of HTLV infection (51). They may simply be a consequence of active Tax expression and vial replication. In our experiments, the nuclear and cytoplasmic changes were more dramatic than those seen in flower cells. This may reflect the regulation of Tax expression by Rex in virus-infected cells.

The disparate effect of cell proliferation and cellular toxicity caused by Tax remains a complex issue. We think the cell cycle dysfunctions are principally responsible for the toxicity of Tax in various cell types. Under the conditions under which the Tax-transduced cells were grown, no significant cellular apoptosis was observed and no features of apoptosis were detected with electron microscopy. Cells with division defects persisted in normal culture medium containing 10 or 20% FBS. They became lost during passage, however. We did not attempt to grow them under the serum-deprived conditions reported to induce apoptosis previously (60).

Ample examples from papovaviruses, adenovirus, and human immunodeficiency virus indicate that activation of G_1/S transition is critical for viral replication in mitotically inert cells. Furthermore, G_2/M cell cycle arrest caused by human

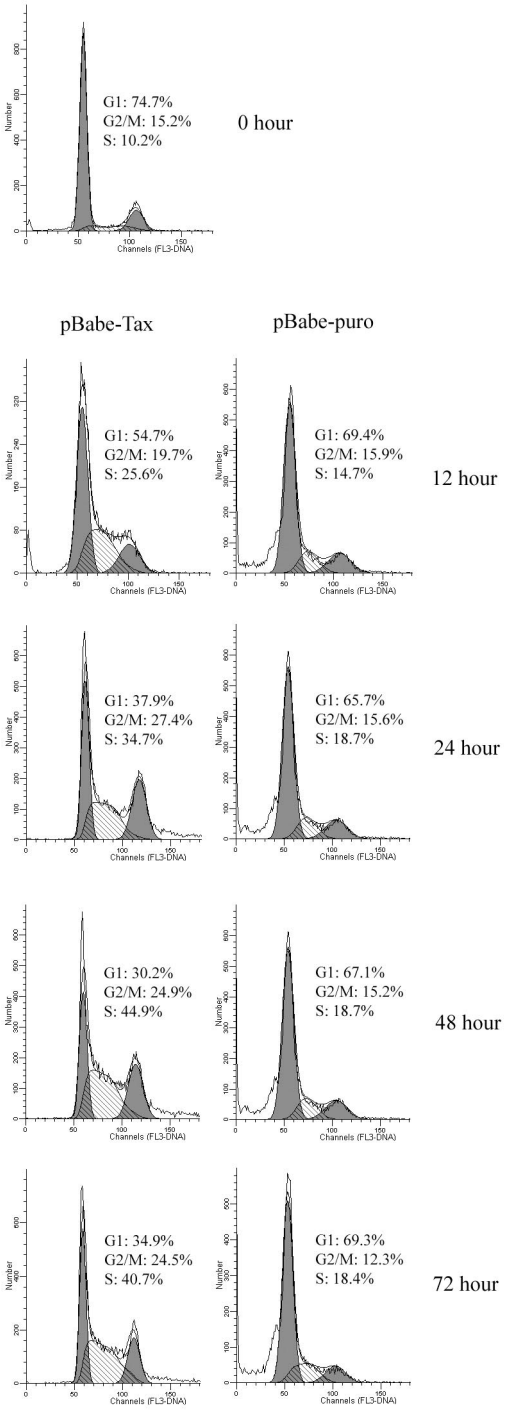

FIG. 8. Kinetics of G_1/S transition and G_2/M arrest caused by Tax. Two million PA18G-BHK-21 cells were serum starved; infected with pBabe-Tax (left panels) or pBabe-puro (right panels) at an MOI of 10; and grown in 20% FBS for 12, 24, 48, and 72 h. Flow cytometry and data analyses were carried out as described in the legend to Fig. 6.

immunodeficiency virus Vpr has been shown to significantly augment viral production (6, 15, 26, 63). We think the cell cycle perturbations brought on by Tax most likely are also consequences of cellular activation necessary for productive viral replication. Presumably, activation of cell cycle entry coupled with inhibition of mitosis by Tax keeps the HTLV-1-infected cells in a metabolically active state for viral replication. The inability of Tax-expressing cells to exit the cell cycle mostly causes the steady decline of Tax expression in the transduced cell population. To extend this line of thinking further, we think HTLV-1-infected T cells that actively produce viral particles in vivo and become arrested at mitosis are not likely to survive. This activity of Tax immediately raises a question regarding PX1 and MT4 cells that produce Tax to high levels. Both cell lines show considerable Tax expression without the accompanying abnormalities in the late stages of cell division cycle. How can the differences between Tax-transduced (NIH 3T3, WI-38, and PA18G-BHK-21) and Tax-transformed (PX1 and MT4) cells be reconciled? It is important to remember that the transformed cells–-MT4 and PX1–-that express Tax have undergone stringent selection in cell culture and in vivo, respectively, and should not be equated to the cultured cells that expressed Tax for the first time after retroviral transduction, as described here. This interesting difference suggests that some cellular changes in transformed cells must have occurred to render Tax expression permissible. We speculate that cell-specific changes in PX1 and MT4 may be responsible for their progress through the cell cycle. Although other HTLV-1 gene products may play a role in cells containing the proviral genome, such as MT4, the ability of PX1 cells to divide indicates that these other viral genes are not required for successful release of the blockade of mitosis. Since PX1 cells are derived from transgenic mouse tumors, the underlying regulatory mechanism may point to an important process related to the pathogenesis of HTLV-1 and the development of adult T-cell leukemia.

What is the biochemical basis for the dramatic cell activation and cell cycle changes caused by Tax? Considering the fact that Tax is capable of interacting with a wide range of cellular proteins, including CREB/ATF-1, CBP, and P/CAF, to activate HTLV-1 transcription, we think equally elaborate protein-protein interactions are likely to mediate its activation of the cell and its interference with the cell cycle. The Tax-mediated activation of G_1/S transition that we observed is consistent with studies showing that Tax activates CDK4 and CDK6 (44, 52) and can trigger interleukin-2-dependent T cells to enter into cell cycle in an interleukin-2-independent manner (46). This function appears to be coincident with the ability of Tax to activate the NF-κB pathway (43). In this sense, we think NF-κB activation may be one facet of a broad and general cellular activation mechanism of Tax. Tax has been shown to induce the expression of the cyclin-dependent kinase inhibitor $p21^{CIP1/WAF1}$ (2, 13). We are in the process of examining the status of various cell cycle regulators in Tax-expressing cells. One explanation for our observations is that Tax activates cells to replicate DNA via a mechanism not fully understood at present, and this constitutive activation, at the same time, results in a block in the completion of mitosis as reflected by an inability of cells to undertake cytokinesis, yet accompanied by multiple rounds of inappropriate DNA synthesis. Further experiments are needed to determine whether the inability to complete mitosis is a necessary consequence of the activation of S-phase entry by Tax.

Jin et al. (25) had previously reported that the interaction

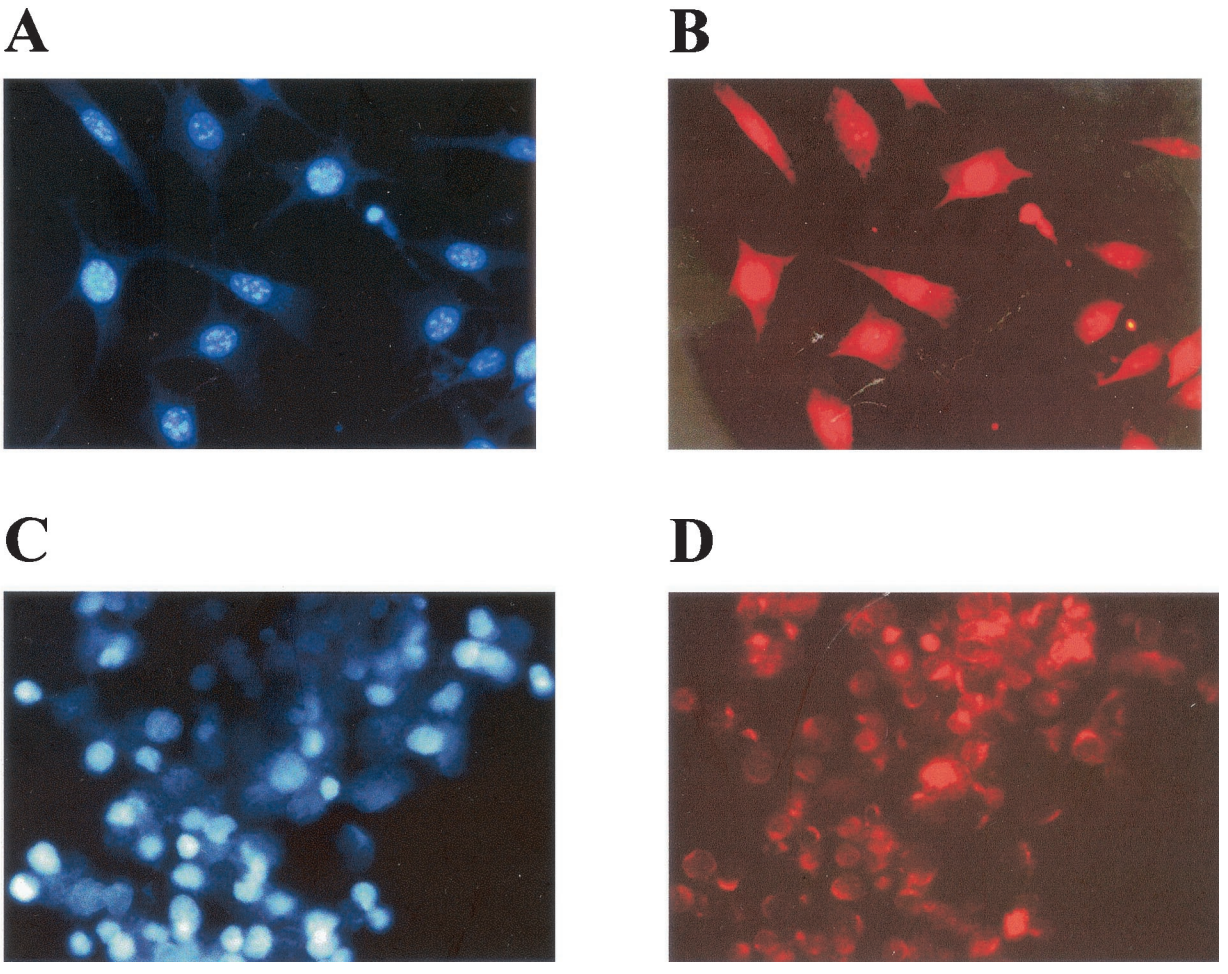

FIG. 9. PX1 and MT4 cells are not multinucleated. DAPI staining (A and C) and Tax immunofluorescence (B and D) analyses for PX1 and MT4 cells, respectively, were carried out as described in the legend to Fig. 3. Note the nuclear speckles (D) and significant cytoplasmic localization of Tax (B and D).

between Tax and hsMAD1 causes a spindle checkpoint defect that was proposed to be the cause of aneuploidy, microsatellite instability, and formation of multinucleated giant cells. Indeed, HeLa cells transfected with a Tax-expressing plasmid form binucleated cells (21, 25). While the Tax-induced block in mitosis may be due to Tax-hsMAD1 interaction and defects in spindle checkpoint control, the fact remains that Tax influences the cell cycle at multiple levels. We have recently found that Tax is a noncompetitive inhibitor of the major serine/threonine phosphatase 2A (unpublished data), which is a major negative regulator of many signaling pathways, including the mitogen-activated protein kinase cascade; DNA replication; transcription; cell cycle progression, including execution of the spindle checkpoint; the IκB kinase signaling pathway; and the TOR (target of rapamycin) kinase signaling pathway (for comprehensive reviews, see references 39 and 22)–-to mention just a few. How the cell cycle changes caused by Tax can be linked to its ability to activate IκB kinase and NF-κB; the interaction of Tax with some of the cell cycle regulators, such as p16, HsMAD1, and serine/threonine phosphatase 2A; or the interaction of Tax with CBP and P/CAF will be a subject of intense interest.

ACKNOWLEDGMENTS

We thank Xin Xiang for assistance with fluorescence microscopy; Viagene, Inc., for the 293GP cell line; Jing-Kuan Yee for the CMV-VSV-G construct; Terese Astier-Gin for the PA18G-BHK-21 cell line; and Yu-liang Kuo for the purified 4C5 Tax antibody.

This work was supported by grants RO1 CA48709 and RO1 CA/GM 75688 from the National Institutes of Health.

REFERENCES

1. **Adya, N., L. J. Zhao, W. Huang, I. Boros, and C. Z. Giam.** 1994. Expansion of CREB's DNA recognition specificity by Tax results from interaction with Ala-Ala-Arg at positions 282–284 near the conserved DNA-binding domain of CREB. Proc. Natl. Acad. Sci. USA **91:**5642–5646.
2. **Akagi, T., H. Ono, and K. Shimotohno.** 1996. Expression of cell-cycle regulatory genes in HTLV-I infected T-cell lines: possible involvement of Tax1 in the altered expression of cyclin D2, p18Ink4 and p21Waf1/Cip1/Sdi1. Oncogene **12:**1645–1652.
3. **Armstrong, A. P., A. A. Franklin, M. N. Uittenbogaard, H. A. Giebler, and J. K. Nyborg.** 1993. Pleiotropic effect of the human T-cell leukemia virus Tax protein on the DNA binding activity of eukaryotic transcription factors. Proc. Natl. Acad. Sci. USA **90:**7303–7307.
4. **Astier-Gin, T., J. P. Portail, F. Lafond, and B. Guillemain.** 1995. Identification of HTLV-I- or HTLV-II-producing cells by cocultivation with BHK-21 cells stably transfected with a LTR-lacZ gene construct. J. Virol. Methods **51:**19–29.
5. **Baranger, A. M., C. R. Palmer, M. K. Hamm, H. A. Giebler, A. Brauweiler, J. K. Nyborg, and A. Schepartz.** 1995. Mechanism of DNA-binding enhance-

ment by the human T-cell leukaemia virus transactivator Tax. Nature **376:** 606–608.
6. **Bartz, S. R., M. E. Rogel, and M. Emerman.** 1996. Human immunodeficiency virus type 1 cell cycle control: Vpr is cytostatic and mediates G_2 accumulation by a mechanism which differs from DNA damage checkpoint control. J. Virol. **70:**2324–2331.
7. **Bex, F., M. J. Yin, A. Burny, and R. B. Gaynor.** 1998. Differential transcriptional activation by human T-cell leukemia virus type 1 Tax mutants is mediated by distinct interactions with CREB binding protein and p300. Mol. Cell. Biol. **18:**2392–2405.
8. **Chlichlia, K., M. Busslinger, M. E. Peter, H. Walczak, P. H. Krammer, V. Schirrmacher, and K. Khazaie.** 1997. ICE-proteases mediate HTLV-I Tax-induced apoptotic T-cell death. Oncogene **14:**2265–2272.
9. **Chlichlia, K., G. Moldenhauer, P. T. Daniel, M. Busslinger, L. Gazzolo, V. Schirrmacher, and K. Khazaie.** 1995. Immediate effects of reversible HTLV-1 tax function: T-cell activation and apoptosis. Oncogene **10:**269–277.
10. **Chu, Z. L., Y. A. Shin, J. M. Yang, J. A. Di Donato, and D. W. Ballard.** 1999. IKKγ mediates the interaction of cellular IκB kinases with the tax transforming protein of human T cell leukemia virus type 1. J. Biol. Chem. **274:**15297–15300.
11. **Copeland, K. F., A. G. Haaksma, J. Goudsmit, P. H. Krammer, and J. L. Heeney.** 1994. Inhibition of apoptosis in T cells expressing human T cell leukemia virus type I Tax. AIDS Res. Hum. Retrovir. **10:**1259–1268.
12. **Datta, S., N. H. Kothari, and H. Fan.** 2000. In vivo genomic footprinting of the human T-cell leukemia virus type 1 (HTLV-1) long terminal repeat enhancer sequences in HTLV-1-infected human T-cell lines with different levels of Tax I activity. J. Virol. **74**:8277–8285.
13. **de La Fuente, C., F. Santiago, S. Y. Chong, L. Deng, T. Mayhood, P. Fu, D. Stein, T. Denny, F. Coffman, N. Azimi, R. Mahieux, and F. Kashanchi.** 2000. Overexpression of $p21^{waf1}$ in human T-cell lymphotropic virus type 1-infected cells and its association with cyclin A/cdk2. J. Virol. **74**:7270–7283.
14. **Grossman, W. J., J. T. Kimata, F. H. Wong, M. Zutter, T. J. Ley, and L. Ratner.** 1995. Development of leukemia in mice transgenic for the tax gene of human T-cell leukemia virus type I. Proc. Natl. Acad. Sci. USA **92:**1057–1061.
15. **Gummuluru, S., and M. Emerman.** 1999. Cell cycle- and Vpr-mediated regulation of human immunodeficiency virus type 1 expression in primary and transformed T-cell lines. J. Virol. **73**:5422–5430.
16. **Haller, K., T. Ruckes, I. Schmitt, D. Saul, E. Derow, and R. Grassmann.** 2000. Tax-dependent stimulation of G_1 phase-specific cyclin-dependent kinases and increased expression of signal transduction genes characterize HTLV type 1-transformed T cells. AIDS Res. Hum. Retrovir. **16**:1683–1688.
17. **Harhaj, E. W., and S. C. Sun.** 1999. IKKγ serves as a docking subunit of the IκB kinase (IKK) and mediates interaction of IKK with the human T-cell leukemia virus Tax protein. J. Biol. Chem. **274**:22911–22914.
18. **Harrod, R., Y. L. Kuo, Y. Tang, Y. Yao, A. Vassilev, Y. Nakatani, and C. Z. Giam.** 2000. p300 and p300/cAMP-responsive element-binding protein associated factor interact with human T-cell lymphotropic virus type-1 Tax in a multi-histone acetyltransferase/activator-enhancer complex. J. Biol. Chem. **275**:11852–11857.
19. **Harrod, R., Y. Tang, C. Nicot, H. S. Lu, A. Vassilev, Y. Nakatani, and C.-Z. Giam.** 1998. An exposed KID-like domain in human T-cell lymphotropic virus type 1 Tax is responsible for the recruitment of coactivators CBP/p300. Mol. Cell. Biol. **18:**5052–5061.
20. **Hinrichs, S. H., M. Nerenberg, R. K. Reynolds, G. Khoury, and G. Jay.** 1987. A transgenic mouse model for human neurofibromatosis. Science **237:**1340–1343.
21. **Iha, H., T. Kasai, K. V. Kibler, Y. Iwanaga, K. Tsurugi, and K. T. Jeang.** 2000. Pleiotropic effects of HTLV type 1 Tax protein on cellular metabolism: mitotic checkpoint abrogation and NF-κB activation. AIDS Res. Hum. Retrovir. **16:**1633–1638.
22. **Janssens, V., and J. Goris.** 2001. Protein phosphatase 2A: a highly regulated family of serine/threonine phosphatases implicated in cell growth and signalling. Biochem. J. **353:**417–439.
23. **Jiang, H., H. Lu, R. L. Schiltz, C. A. Pise-Masison, V. V. Ogryzko, Y. Nakatani, and J. N. Brady.** 1999. PCAF interacts with Tax and stimulates Tax transactivation in a histone acetyltransferase-independent manner. Mol. Cell. Biol. **19:**8136–8145.
24. **Jin, D. Y., V. Giordano, K. V. Kibler, H. Nakano, and K. T. Jeang.** 1999. Role of adapter function in oncoprotein-mediated activation of NF-κB. Human T-cell leukemia virus type I Tax interacts directly with IκB kinase gamma. J. Biol. Chem. **274:**17402–17405.
25. **Jin, D. Y., F. Spencer, and K. T. Jeang.** 1998. Human T cell leukemia virus type 1 oncoprotein Tax targets the human mitotic checkpoint protein MAD1. Cell **93:**81–91.
26. **Jowett, J. B., V. Planelles, B. Poon, N. P. Shah, M. L. Chen, and I. S. Chen.** 1995. The human immunodeficiency virus type 1 *vpr* gene arrests infected T cells in the G_2+M phase of the cell cycle. J. Virol. **69:**6304–6313.
27. **Kao, S. Y., F. J. Lemoine, and S. J. Marriott.** 2000. Suppression of DNA repair by human T cell leukemia virus type 1 Tax is rescued by a functional p53 signaling pathway. J. Biol. Chem. **275:**35926–35931.
28. **Kimzey, A. L., and W. S. Dynan.** 1999. Identification of a human T-cell leukemia virus type I tax peptide in contact with DNA. J. Biol. Chem. **274:**34226–34232.
29. **Kimzey, A. L., and W. S. Dynan.** 1998. Specific regions of contact between human T-cell leukemia virus type I Tax protein and DNA identified by photocross-linking. J. Biol. Chem. **273:**13768–13775.
30. **Kinoshita, K., T. Amagasaki, S. Ikeda, J. Suzuyama, K. Toriya, K. Nishino, M. Tagawa, M. Ichimaru, S. Kamihira, Y. Yamada, et al.** 1985. Preleukemic state of adult T cell leukemia: abnormal T lymphocytosis induced by human adult T cell leukemia-lymphoma virus. Blood **66:**120–127.
31. **Kwok, R. P., M. E. Laurance, J. R. Lundblad, P. S. Goldman, H. Shih, L. M. Connor, S. J. Marriott, and R. H. Goodman.** 1996. Control of cAMP-regulated enhancers by the viral transactivator Tax through CREB and the co-activator CBP. Nature **380:**642–646.
32. **Lemasson, I., S. Thebault, C. Sardet, C. Devaux, and J. M. Mesnard.** 1998. Activation of E2F-mediated transcription by human T-cell leukemia virus type I Tax protein in a p16(INK4A)-negative T-cell line. J. Biol. Chem. **273:**23598–23604.
33. **Lemoine, F. J., S. Y. Kao, and S. J. Marriott.** 2000. Suppression of DNA repair by HTLV type 1 Tax correlates with Tax *trans*-activation of proliferating cell nuclear antigen gene expression. AIDS Res. Hum. Retrovir. **16:** 1623–1627.
34. **Lenzmeier, B. A., H. A. Giebler, and J. K. Nyborg.** 1998. Human T-cell leukemia virus type I Tax requires direct access to DNA for recruitment of CREB binding protein to the viral promoter. Mol. Cell. Biol. **18:**721–731.
35. **Low, K. G., L. F. Dorner, D. B. Fernando, J. Grossman, K. T. Jeang, and M. J. Comb.** 1997. Human T-cell leukemia virus type 1 Tax releases cell cycle arrest induced by $p16^{INK4a}$. J. Virol. **71:**1956–1962.
36. **Lundblad, J. R., R. P. Kwok, M. E. Laurance, M. S. Huang, J. P. Richards, R. G. Brennan, and R. H. Goodman.** 1998. The human T-cell leukemia virus-1 transcriptional activator Tax enhances cAMP-responsive element-binding protein (CREB) binding activity through interactions with the DNA minor groove. J. Biol. Chem. **273:**19251–19259.
37. **Majone, F., and K. T. Jeang.** 2000. Clastogenic effect of the human T-cell leukemia virus type I Tax oncoprotein correlates with unstabilized DNA breaks. J. Biol. Chem. **275:**32906–32910.
38. **Majone, F., O. J. Semmes, and K. T. Jeang.** 1993. Induction of micronuclei by HTLV-I Tax: a cellular assay for function. Virology **193:**456–459.
39. **Millward, T. A., S. Zolnierowicz, and B. A. Hemmings.** 1999. Regulation of protein kinase cascades by protein phosphatase 2A. Trends Biochem. Sci. **24:**186–191.
40. **Miyoshi, I., I. Kubonishi, S. Yoshimoto, T. Akagi, Y. Ohtsuki, Y. Shiraishi, K. Nagata, and Y. Hinuma.** 1981. Type C virus particles in a cord T-cell line derived by co-cultivating normal human cord leukocytes and human leukaemic T cells. Nature **294:**770–771.
41. **Morgenstern, J. P., and H. Land.** 1990. Advanced mammalian gene transfer: high titre retroviral vectors with multiple drug selection markers and a complementary helper-free packaging cell line. Nucleic Acids Res. **18:**3587–3596.
42. **Nerenberg, M., S. H. Hinrichs, R. K. Reynolds, G. Khoury, and G. Jay.** 1987. The tat gene of human T-lymphotropic virus type 1 induces mesenchymal tumors in transgenic mice. Science **237:**1324–1329.
43. **Neuveut, C., and K. T. Jeang.** 2000. HTLV-I Tax and cell cycle progression. Prog. Cell Cycle Res. **4:**157–162.
44. **Neuveut, C., K. G. Low, F. Maldarelli, I. Schmitt, F. Majone, R. Grassmann, and K.-T. Jeang.** 1998. Human T-cell leukemia virus type 1 Tax and cell cycle progression: role of cyclin D-cdk and p110Rb. Mol. Cell. Biol. **18**:3620–3632.
45. **Nicot, C., F. Tie, and C.-Z. Giam.** 1998. Cytoplasmic forms of human T-cell leukemia virus type 1 Tax induce NF-κB activation. J. Virol. **72:**6777–6784.
46. **Ohtani, K., R. Iwanaga, M. Arai, Y. Huang, Y. Matsumura, and M. Nakamura.** 2000. Cell type-specific E2F activation and cell cycle progression induced by the oncogene product Tax of human T-cell leukemia virus type I. J. Biol. Chem. **275:**11154–11163.
47. **Paca-Uccaralertkun, S., L. J. Zhao, N. Adya, J. V. Cross, B. R. Cullen, I. M. Boros, and C. Z. Giam.** 1994. In vitro selection of DNA elements highly responsive to the human T-cell lymphotropic virus type I transcriptional activator, Tax. Mol. Cell. Biol. **14:**456–462.
48. **Perini, G., S. Wagner, and M. R. Green.** 1995. Recognition of bZIP proteins by the human T-cell leukaemia virus transactivator Tax. Nature **376:**602–605.
49. **Pise-Masison, C. A., K.-S. Choi, M. Radonovich, J. Dittmer, S.-J. Kim, and J. N. Brady.** 1998. Inhibition of p53 transactivation function by the human T-cell lymphotropic virus type 1 Tax protein. J. Virol. **72**:1165–1170.
50. **Pozzatti, R., J. Vogel, and G. Jay.** 1990. The human T-lymphotropic virus type I *tax* gene can cooperate with the *ras* oncogene to induce neoplastic transformation of cells. Mol. Cell. Biol. **10:**413–417.
51. **Sacher, R. A., N. L. Luban, D. I. Ameti, S. Friend, G. B. Schreiber, and E. L. Murphy.** 1999. Low prevalence of flower cells in USA blood donors infected with human T-lymphotrophic virus types I and II. Br. J. Haematol. **105:**758–763.
52. **Schmitt, I., O. Rosin, P. Rohwer, M. Gossen, and R. Grassmann.** 1998. Stimulation of cyclin-dependent kinase activity and G_1- to S-phase transition in human lymphocytes by the human T-cell leukemia/lymphotropic virus type 1 Tax protein. J. Virol. **72**:633–640.

53. **Semmes, O. J., F. Majone, C. Cantemir, L. Turchetto, B. Hjelle, and K. T. Jeang.** 1996. HTLV-I and HTLV-II Tax: differences in induction of micronuclei in cells and transcriptional activation of viral LTRs. Virology **217:**373–379.
54. **Shimoyama, M.** 1991. Diagnostic criteria and classification of clinical subtypes of adult T-cell leukaemia-lymphoma. A report from the Lymphoma Study Group (1984–87). Br. J. Haematol. **79:**428–437.
55. **Suzuki, T., J. I. Fujisawa, M. Toita, and M. Yoshida.** 1993. The transactivator tax of human T-cell leukemia virus type 1 (HTLV-1) interacts with cAMP-responsive element (CRE) binding and CRE modulator proteins that bind to the 21-base-pair enhancer of HTLV-1. Proc. Natl. Acad. Sci. USA **90:**610–614.
56. **Suzuki, T., T. Narita, M. Uchida-Toita, and M. Yoshida.** 1999. Down-regulation of the INK4 family of cyclin-dependent kinase inhibitors by tax protein of HTLV-1 through two distinct mechanisms. Virology **259**:384–391.
57. **Taguchi, H., and I. Miyoshi.** 1983. Three cases of pre-adult T-cell leukemia. Jpn. J. Clin. Oncol. **13**(Suppl. 2)**:**209–214.
58. **Tang, Y., F. Tie, I. Boros, R. Harrod, M. Glover, and C. Z. Giam.** 1998. An extended alpha-helix and specific amino acid residues opposite the DNA-binding surface of the cAMP response element binding protein basic domain are important for human T cell lymphotropic retrovirus type I Tax binding. J. Biol. Chem. **273:**27339–27346.
59. **Wagner, S., and M. R. Green.** 1993. HTLV-I Tax protein stimulation of DNA binding of bZIP proteins by enhancing dimerization. Science **262:**395–399.
60. **Yamada, T., S. Yamaoka, T. Goto, M. Nakai, Y. Tsujimoto, and M. Hatanaka.** 1994. The human T-cell leukemia virus type I Tax protein induces apoptosis which is blocked by the Bcl-2 protein. J. Virol. **68:**3374–3379.
61. **Yamaoka, S., G. Courtois, C. Bessia, S. T. Whiteside, R. Weil, F. Agou, H. E. Kirk, R. J. Kay, and A. Israel.** 1998. Complementation cloning of NEMO, a component of the IκB kinase complex essential for NF-κB activation. Cell **93**:1231–1240.
62. **Yamaoka, S., H. Inoue, M. Sakurai, T. Sugiyama, M. Hazama, T. Yamada, and M. Hatanaka.** 1996. Constitutive activation of NF-kappa B is essential for transformation of rat fibroblasts by the human T-cell leukemia virus type I Tax protein. EMBO J. **15:**873–887.
63. **Yao, X. J., A. J. Mouland, R. A. Subbramanian, J. Forget, N. Rougeau, D. Bergeron, and E. A. Cohen.** 1998. Vpr stimulates viral expression and induces cell killing in human immunodeficiency virus type 1-infected dividing Jurkat T cells. J. Virol. **72**:4686–4693.
64. **Yee, J. K., A. Miyanohara, P. LaPorte, K. Bouic, J. C. Burns, and T. Friedmann.** 1994. A general method for the generation of high-titer, pantropic retroviral vectors: highly efficient infection of primary hepatocytes. Proc. Natl. Acad. Sci. USA **91:**9564–9568.
65. **Yin, M. J., and R. B. Gaynor.** 1996. Complex formation between CREB and Tax enhances the binding affinity of CREB for the human T-cell leukemia virus type 1 21-base-pair repeats. Mol. Cell. Biol. **16:**3156–3168.
66. **Yin, M. J., and R. B. Gaynor.** 1996. HTLV-1 21 bp repeat sequences facilitate stable association between Tax and CREB to increase CREB binding affinity. J. Mol. Biol. **264:**20–31.
67. **Yin, M. J., E. Paulssen, J. Seeler, and R. B. Gaynor.** 1995. Chimeric proteins composed of Jun and CREB define domains required for interaction with the human T-cell leukemia virus type 1 Tax protein. J. Virol. **69:**6209–6218.
68. **Zhao, L. J., and C. Z. Giam.** 1991. Interaction of the human T-cell lymphotropic virus type I (HTLV-I) transcriptional activator Tax with cellular factors that bind specifically to the 21-base-pair repeats in the HTLV-I enhancer. Proc. Natl. Acad. Sci. USA **88:**11445–11449.
69. **Zhao, L. J., and C. Z. Giam.** 1992. Human T-cell lymphotropic virus type I (HTLV-I) transcriptional activator, Tax, enhances CREB binding to HTLV-I 21-base-pair repeats by protein-protein interaction. Proc. Natl. Acad. Sci. USA **89:**7070–7074.